

On the Source of Jitter in a Room-Temperature Nanoinjection Photon Detector at $1.55 \mu\text{m}$

Omer Gokalp Memis, Alex Katsnelson, Hooman Mohseni, Minjun Yan, Shuang Zhang, Tim Hossain, Niu Jin, and Ilesanmi Adesida

Abstract—The transient response of a nanoinjection infrared photon detector was studied by exploring the relation between lateral charge transfer and jitter. The jitter of the device was measured to be 15 ps at room temperature. The jitter was almost independent of the pulse power, even after device saturation. Spatial maps for delay and amplitude were acquired. The carrier velocity was extracted from the measurements and compared with that of the simulation model. The jitter due to transit time was calculated to be in agreement with the measured data, which indicated that the jitter is primarily transit time limited.

Index Terms—Jitter, lateral transport, nanoinjection, photon detector.

I. INTRODUCTION

AS THE speed of computing increases at a growing pace, many modern applications require fast, secure, and error-free communications to cope with the vast amounts of transmitted data. In parallel to these demands, the telecommunication industry increases the bit rates and therefore requires faster and more sensitive detectors with low jitter [1]. These fast sensitive detectors, when coupled with an internal amplification mechanism, can also help in the development of emerging technologies and the improvement of existing technologies. Novel applications such as quantum key distribution [2] and quantum cryptography [3] require detectors with high signal-to-noise ratio, fast response, and low jitter.

Current technologies for short-wave infrared photon detection are InGaAs p-i-n detectors [4], InGaAs/InP avalanche photodetectors (APDs) [5], and superconducting photon detectors [6]. InGaAs p-i-n diodes have very low leakage current and noise levels with high timing resolution (low jitter). However, they do not have an internal gain mechanism, and the overall noise level and jitter are limited by the proceeding electronics. InGaAs/InP APDs, which have internal amplification, have

been developed for short-wave infrared beyond $1 \mu\text{m}$. They were inspired by the success of Si APDs in the visible domain [7]. In Geiger mode, the InGaAs/InP APDs have jitter values of about 50 ps with single photons, and researchers have reported achieving 30 ps with some tradeoffs [8]. Studies have also shown that jitter in InGaAs/InP APDs decreases when the optical flux [9] is higher, and to compare, an improvement factor of 3–7 [3], [10] in time resolution has been reported for Si APDs when the optical flux was increased by three orders of magnitude. Superconducting detectors have well-defined time resolutions, even with a single photon, and the lowest reported jitter values are about 18 ps [11] and -30 ps [12] at temperatures of less than 10 K.

As an alternative to these technologies, we have developed a short-wave infrared photodetector based on carrier focalization and nanoinjection [13]. The detection mechanism is based on amplification in and injection from nanometer-scale pillars, i.e., “nanoinjectors,” toward a large InGaAs absorption volume. The details of the device geometry, growth, and fabrication have been reported in [13]. Recently, we have demonstrated the stability of the internal amplification mechanism, with the resulting low statistical variation and reduced noise levels. Experimentally, the earlier devices have provided gain values of up to 10 000 while exhibiting sub-Poissonian (suppressed) noise levels with fano factors of as low as 0.55. However, the transient response has been slow, which we have attributed to a lack of surface passivation. Here, we report on the high-speed response, delay, and jitter performance of the devices with surface passivation.

II. EXPERIMENTAL RESULT

The devices were passivated with polyimide. Using the passivated devices, we have studied the reasons for delays and jitter. We have initially theorized that the time uncertainty of the amplification method would be low and that the devices would show a low jitter at room temperature. We believed that the origin of jitter lies in the charge transport delay. Based on our design, we have predicted that the transient delay would be due to lateral charge transport in the InGaAs absorption volume, and the jitter would primarily be caused by the differences in transit time in the InGaAs absorption volume [Fig. 1(a)].

To evaluate our predictions, the nanoinjection detectors were tested in a custom-designed setup that is capable of calibrated infrared illumination, visible/infrared imaging, and motorized scanning. High-frequency RF probes were connected to individual devices and performed measurements. The detectors

Manuscript received March 25, 2008. The work of H. Mohseni was supported in part by the National Science Foundation and in part by the Defense Advanced Research Projects Agency. The work of I. Adesida was supported by the Defense Advanced Research Projects Agency. The review of this letter was arranged by Editor P. K.-L. Yu.

O. G. Memis, A. Katsnelson, and H. Mohseni are with the Department of Electrical Engineering and Computer Science, Northwestern University, Evanston, IL 60208 USA (e-mail: gokalp@northwestern.edu; a-katsnelson@northwestern.edu; hmohseni@eecs.northwestern.edu).

M. Yan, S. Zhang, T. Hossain, N. Jin, and I. Adesida are with the Micro and Nanotechnology Laboratory, University of Illinois at Urbana-Champaign, Urbana, IL 61801 USA (e-mail: myan@uiuc.edu; zhangs75@gmail.com; tim.hossain@gmail.com; jin.niu@gmail.com; iadesida@uiuc.edu).

Color versions of one or more of the figures in this letter are available online at <http://ieeexplore.ieee.org>.

Digital Object Identifier 10.1109/LED.2008.2001123

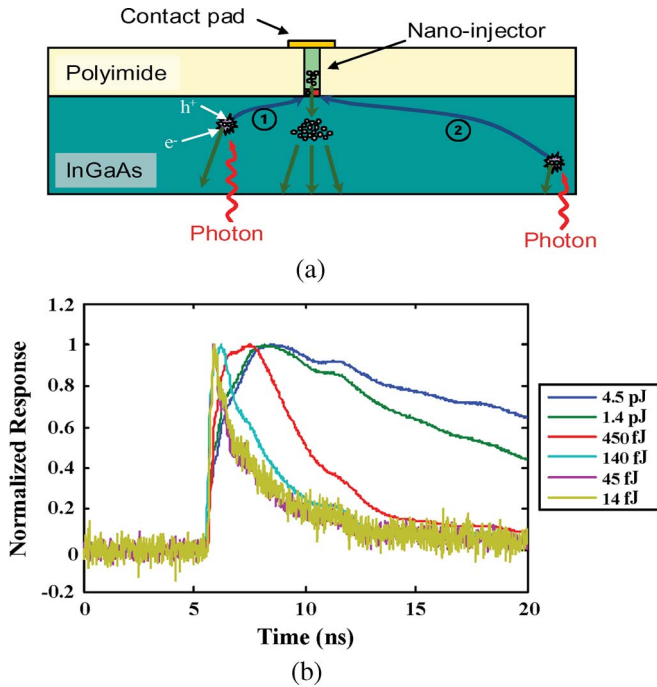


Fig. 1. (a) Cross section of the device. Different carrier paths in the device result in different transport times. (b) Normalized transient response of the device over a large dynamic range of pulse energy (averaged) of 14 fJ–2.2 pJ.

were biased using a low-noise dc power supply fed through a bias tee. A femtosecond pulsed laser with a jitter of < 70 fs was attenuated and focused onto the devices using a near-infrared-response microscope setup. Equipped with remotely controllable actuators, the setup has the capability of scanning the sample to map the spatial dependence of parameters. The RF signal coming from the devices was extracted using the bias tee and amplified by a low-noise amplifier (LNA) with 2.4-dB noise figure, 2.5-GHz nominal bandwidth, and 9-ps jitter. The amplified signal was then acquired by the high-speed sampling oscilloscope Agilent 86100C (with a jitter of 1.7 ps), which directly measured the delay, rise time, and jitter. The timing signal was generated by a low-jitter (1.2-ps) p-i-n detector connected to the second output port of the laser.

The fabricated devices had a layer structure of 1000-nm InGaAs, 50-nm GaAsSb, 50-nm InAlAs, and 500-nm InP from bottom to top. After dry etching, the samples were passivated with polyimide with a thickness of 500 nm. The tested devices had an injector radius of $1 \mu\text{m}$ and were chosen because of their larger signal-to-noise ratios, compared to submicrometer devices. The devices were illuminated with a 300-fs pulsed fiber laser with 20-MHz repetition rate and 1.4-pJ pulse energy after 10 dB of attenuation. The corresponding rise time at 1-V bias was 200 ps, with a jitter of 15 ps. To see the effect of optical saturation, the power was increased to 14 pJ, where the pulse shape exhibits compression [Fig. 1(b)]. The compressed response was compared to the results without the LNA in the signal path to verify that the source of compression was indeed the nano-injection detector. Measurements of nominal rms jitter with an increased pulse intensity stayed stable at about 15 ps, indicating that there was no significant change of the jitter.

To evaluate the transit time, the $2\text{-}\mu\text{m}$ laser spot was scanned using motorized drivers, and a map of the delay around the

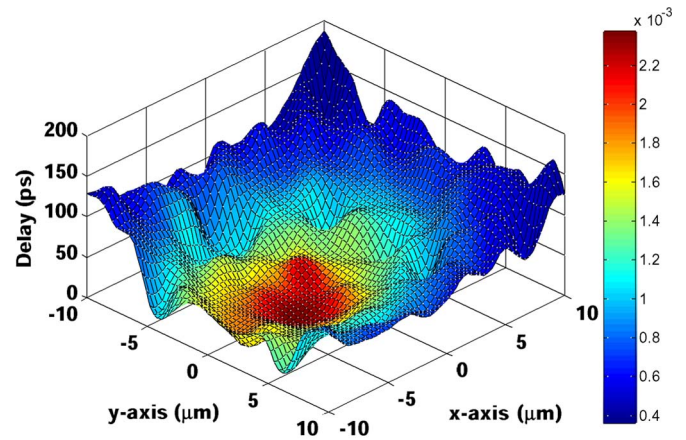


Fig. 2. Delay–amplitude map of the detector. The z -axis (height) corresponds to the measured delay, and the color coding corresponds to the measured peak current (in amperes). The map was corrected for the changes in pulse shape.

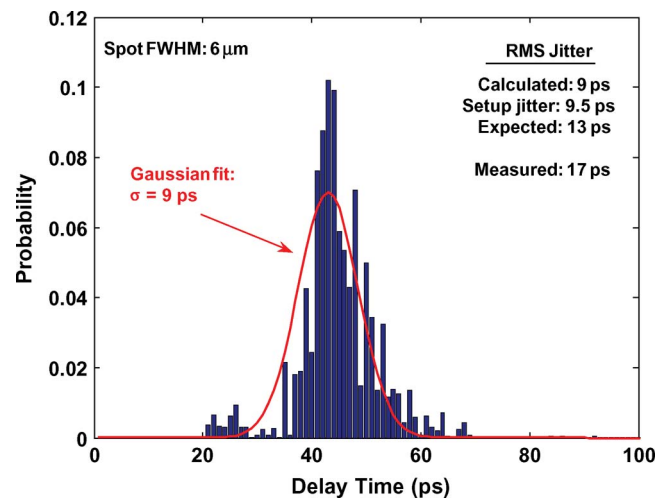


Fig. 3. Probability distribution for the carrier arrival times, using the information from the delay map. The illumination spot size is $6 \mu\text{m}$. The estimated rms jitter is 9 ps, the estimated jitter with the measurement setup jitter added was 13 ps, and the measured value is 17 ps.

device was extracted, together with the amplitude of the response. Measurements indicate that the active area of the device for pulsed illumination extended to $8\text{--}9 \mu\text{m}$ away from the nanoinjectors (Fig. 2). The effective carrier velocity around the nanoinjector was calculated as $7 \cdot 10^4$ m/s. In order to evaluate the results, we used a 3-D nonlinear finite-element-method-based simulation model. This model has previously shown good agreement with the measured low-frequency response of the device [13]. The electric field, carrier density, and current density distributions inside the device were calculated. The estimated drift velocity was found to be $4 \cdot 10^4$ m/s. The carrier diffusion velocity was about $2 \cdot 10^4$ m/s in the opposite direction, due to the focalization and compression of holes and the elevated carrier density around the center.

The jitter performance was also evaluated using the measured delay and amplitude maps. A variable illumination spot size was assumed, and the spatial generation of carriers and corresponding transit delays was modeled and analyzed in

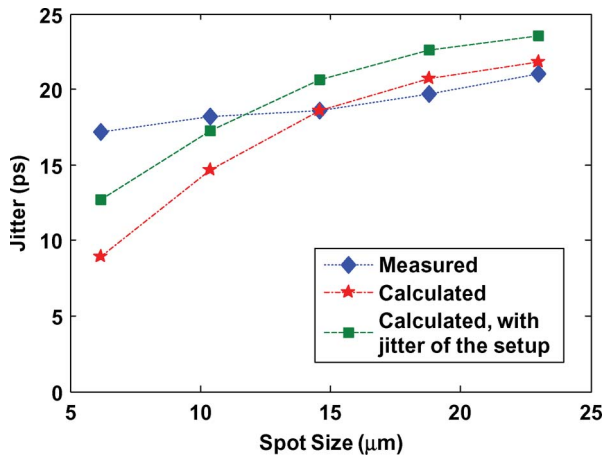


Fig. 4. Effect of spot size on jitter. (Diamond) Measured rms jitter. (Star) Expected jitter values calculated from the 2-D delay maps. (Square) Calculated values with the measurement setup jitter added.

Matlab. The expected jitter was calculated using the probability distribution for carrier arrival times (Fig. 3). The jitter was predicted to be 9 ps for a 6- μm spot size, 19 ps for a 15- μm diameter, and 22 ps for a 24- μm diameter.

In parallel with the theorized delay–jitter relation and calculations, the laser was defocused to see and experimentally quantify the effect of spot size on jitter. The spot size was calculated using the deviation from the focal plane and the numerical aperture of the focusing lens. The values showed a monotonically increasing trend, with larger spot sizes ranging from 17 ps for the smallest spot sizes to 22 ps for a 24- μm spot diameter (Fig. 4). The increase is mainly due to the larger optical generation area.

The values obtained from direct jitter measurements well match with the jitter predictions from delay measurements, particularly at larger spot sizes. These results suggest that the jitter is mostly due to transit time, confirming our predictions regarding the stable nature of nano-injection-based amplification in the time domain.

For small spot sizes, the calculated values were smaller than the measured values, even when the jitter of the measurement setup was considered. We believe this is primarily due to device saturation. We have observed the effects of saturation in pulse shapes [Fig. 1(b)], which create an apparent increase in delay due to the increase in rise times. A similar increase manifests itself for small spot sizes in the vicinity of the injector, where the pulses saturate the device due to the larger local amplitude response. Hence, a rather flat delay–distance relationship around the center of the device is observed, instead of the expected concave shape, and the jitter values are underestimated in the calculations for small spot sizes. This phenomenon agrees with the overestimated effective carrier velocity around the center of the device (measured carrier velocity of $7 \cdot 10^4$ m/s versus expected carrier velocity of $2 \cdot 10^4$ m/s), which was also due to the flat region in spatial delay maps.

III. CONCLUSION

We have quantified the jitter and delay relation in the transient response of a nano-injection infrared photon detector. The room-temperature jitter was measured as 15–18 ps over a broad dynamic range from low-energy pulses to intensity beyond device saturation. The spatial maps for delay and amplitude were acquired and used to compare the measured carrier velocity of $7 \cdot 10^4$ m/s to the simulation predictions. The delay histogram was extracted from delay maps, and expected rms jitter values were calculated under different illumination spot sizes ranging from 6 to 24 μm , and the jitter predictions from the delay maps well matched with the actual jitter measurements, particularly at large spot sizes. The time stability of nano-injection-based amplification, which we theorized during the design of the nano-injection detector, was experimentally verified.

REFERENCES

- [1] S. Sunter and A. Roy, “On-chip digital jitter measurement, from megahertz to gigahertz,” *IEEE Des. Test. Comput.*, vol. 21, no. 4, pp. 314–321, Jul./Aug. 2004.
- [2] R. T. Thew, S. Tanzilli, L. Krainer, S. C. Zeller, A. Rochas, I. Rech, S. Cova, H. Zbinden, and N. Gisin, “Low jitter up-conversion detectors for telecom wavelength GHz QKD,” *New J. Phys.*, vol. 8, p. 32, Mar. 2006.
- [3] I. Prochazka, K. Hamal, and B. Sopko, “Recent achievements in single photon detectors and their applications,” *J. Mod. Opt.*, vol. 51, no. 9/10, pp. 1289–1313, Jun. 2004.
- [4] A. Poloczek, M. Weiss, S. Fedderwitz, A. Stoehr, W. Prost, D. Jaeger, and F. J. Tegude, “Integrated InGaAs pin-diode on exactly oriented silicon (001) substrate suitable for 10 Gbit/s digital applications,” in *Proc. 20th Annu. Meeting IEEE LEOS*, 2007, pp. 180–181.
- [5] S. Cova, M. Ghioni, A. Lotito, I. Rech, and F. Zappa, “Evolution and prospects for single-photon avalanche diodes and quenching circuits,” *J. Mod. Opt.*, vol. 51, no. 9/10, pp. 1267–1288, Jun. 2004.
- [6] S. Somani, S. Kasapi, K. Wilsher, W. Lo, R. Sobolewski, and G. Gol’tsman, “New photon detector for device analysis: Superconducting single-photon detector based on a hot electron effect,” *J. Vac. Sci. Technol. B, Microelectron. Nanometer Struct.*, vol. 19, no. 6, pp. 2766–2769, 2001.
- [7] M. Ghioni, A. Gulinatti, I. Rech, F. Zappa, and S. Cova, “Progress in silicon single-photon avalanche diodes,” *IEEE J. Sel. Topics Quantum Electron.*, vol. 13, no. 4, pp. 852–862, Jul./Aug. 2007.
- [8] M. A. Itzler, R. Ben-Michael, C. F. Hsu, K. Slomkowski, A. Tosi, S. Cova, F. Zappa, and R. Ispasoiu, “Single photon avalanche diodes (SPADs) for 1.5 μm photon counting applications,” *J. Mod. Opt.*, vol. 54, no. 2, pp. 283–304, Jan. 2007.
- [9] M. G. Liu, C. Hu, X. G. Bai, X. Y. Guo, J. C. Campbell, Z. Pan, and M. M. Tashima, “High-performance InGaAs/InP single-photon avalanche photodiode,” *IEEE J. Sel. Topics Quantum Electron.*, vol. 13, no. 4, pp. 887–894, Jul./Aug. 2007.
- [10] J. Blazej, “Photon number resolving in Geiger mode avalanche photodiode photon counters,” *J. Mod. Opt.*, vol. 51, no. 9/10, pp. 1491–1497, Jun. 2004.
- [11] A. Pearlman, A. Cross, W. Slysz, J. Zhang, A. Verevkin, M. Currie, A. Korneev, P. Kouminov, K. Smirnov, B. Voronov, G. Gol’tsman, and R. Sobolewski, “Gigahertz counting rates of NbN single-photon detectors for quantum communications,” *IEEE Trans. Appl. Supercond.*, vol. 15, no. 2, pp. 579–582, Jun. 2005.
- [12] E. A. Dauler, B. S. Robinson, A. J. Kerman, J. K. W. Yang, K. M. Rosfjord, V. Anant, B. Voronov, G. Gol’tsman, and K. K. Berggren, “Multi-element superconducting nanowire single-photon detector,” *IEEE Trans. Appl. Supercond.*, vol. 17, no. 2, pp. 279–284, Jun. 2007.
- [13] O. G. Memis, A. Katsnelson, S. C. Kong, H. Mohseni, M. Yan, S. Zhang, T. Hossain, N. Jin, and I. Adesida, “A photon detector with very high gain at low bias and at room temperature,” *Appl. Phys. Lett.*, vol. 91, no. 17, p. 171 112, Oct. 2007.